

Magnetic Levitation To Characterize the Kinetics of Free-Radical Polymerization

Shencheng Ge,[†] Sergey N. Semenov,[†] Amit A. Nagarkar,[†] Jonathan Milette,[†] Dionysios C. Christodouleas,[†] Li Yuan,[†] and George M. Whitesides^{*,†,‡,§,Ⓜ}

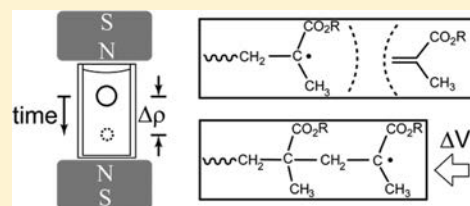
[†]Department of Chemistry & Chemical Biology, Harvard University, 12 Oxford Street, Cambridge, Massachusetts 02138, United States

[‡]Wyss Institute for Biologically Inspired Engineering, Harvard University, 60 Oxford Street, Cambridge, Massachusetts 02138, United States

[§]Kavli Institute for Bionano Science & Technology, Harvard University, 29 Oxford Street, Cambridge, Massachusetts 02138, United States

Supporting Information

ABSTRACT: This work describes the development of magnetic levitation (MagLev) to characterize the kinetics of free-radical polymerization of water-insoluble, low-molecular-weight monomers that show a large change in density upon polymerization. MagLev measures density, and certain classes of monomers show a large change in density when monomers covalently join in polymer chains. MagLev characterized both the thermal polymerization of methacrylate-based monomers and the photopolymerization of methyl methacrylate and made it possible to determine the orders of reaction and the Arrhenius activation energy of polymerization. MagLev also made it possible to monitor polymerization in the presence of solids (aramid fibers, and carbon fibers, and glass fibers). MagLev offers a new analytical technique to materials and polymer scientists that complements other methods (even those based on density, such as dilatometry), and will be useful in investigating polymerizations, evaluating inhibition of polymerizations, and studying polymerization in the presence of included solid materials (e.g., for composite materials).



INTRODUCTION

This work describes the use of magnetic levitation (MagLev) to measure changes in density, $\Delta\rho$, and thus to characterize the kinetics of polymerization, especially free-radical polymerization of water-insoluble, low-molecular-weight monomers. An unmet need in the field of polymer chemistry is for low-cost, easy-to-use, and robust analytical tools that can quantitatively and rapidly measure the kinetics of free-radical polymerization for a range of monomers. In particular, a benchtop tool that is compatible with small quantities of samples and different physical forms of samples—ranging from low-viscosity liquids to solids—would be useful in the early stages of synthesis of new polymers, for characterizing activities of inhibitors and initiators, and for studying mechanisms of polymerization.

Polymer science has developed a number of analytical techniques to monitor the kinetics of polymerization reactions. Operationally, and in terms of sophistication/expense, those techniques fall into two broad categories: (i) One category comprises techniques requiring high-end instrumentation,¹ such as rheometry, calorimetry, gel-permeation chromatography, various forms of UV/vis spectroscopy, mass spectrometry, and NMR spectroscopy. These techniques, individually or in combination (as, for example in automatic continuous online monitoring of polymerization reactions^{1,2})

can give extraordinary detail, but are expensive to acquire and maintain. (ii) The second category uses less sophisticated analytical tools such as balances, refractometers, Ostwald viscometers, and dilatometers.^{3–6} These benchtop tools are easily accessible in research laboratories and at quality-control stations. Of the techniques available, dilatometry (which measures volume and assumes constant mass, and thus effectively measures density) is closest to the MagLev techniques—which we describe here—that measure density directly.

Historically, volume dilatometry has played an important role in characterizing the kinetics of free-radical polymerization. It measures the volumetric shrinkage of a sample of polymer and monomer (as the monomers move from a van der Waals distance in liquid monomer to a covalent and shorter distance in polymer), and hence the kinetics of its polymerization. It is broadly compatible with polymer systems that shrink (or expand) in volume during polymerization (e.g., bulk, suspension, emulsion polymerization of monomers containing vinyl groups). With appropriate modifications, it can also be used to study photopolymerization.⁷

Received: October 12, 2017

Published: December 6, 2017

Volume dilatometry has at least three major shortcomings: (i) It normally requires large volumes of samples (e.g., 1–10 mL), and is thus not applicable to monomers available in limited quantities (<100 μL). (ii) It monitors polymerization for samples of monomers that are directly placed in the dilatometer, and is thus not useful as a stand-alone device to monitor polymerization in another reaction vessel. (iii) It is generally limited to the early stages of polymerization (before the reaction mixture becomes tacky, or solidifies, and clings to the vessel wall, thus preventing reliable readings of positions of the meniscus.

This work demonstrates that MagLev provides a convenient and robust benchtop technique well suited to characterize—quantitatively and rapidly—the kinetics of polymerization of water-insoluble, low-molecular-weight monomers that show a large change in density during polymerization. The method may be particularly useful for quality control, exploratory studies, and screenings of radical polymerization in the presence of included water-insoluble solids (e.g., glass fibers, carbon fibers, and aluminum meshes). It should also be useful in instructional laboratories. The work is based on the change in density (usually an increase) that often accompanies polymerization for certain classes of monomers, especially for low-molecular-weight vinyl monomers.

MagLev has seven useful characteristics as a method to monitor the kinetics of polymerizations: (i) It is a label-free technique (by monitoring the changes in density). (ii) It can conveniently monitor the polymerization in real time over its entire course of polymerization (including the “gel” region). (iii) It provides an isothermal environment for the polymerizing sample. (iv) It can monitor polymerization in the presence of a range of diamagnetic solid materials. (v) It requires small quantities of samples. (vi) It performs non-destructive measurements (samples can be retrieved for further analyses). (vii) It is inexpensive and portable, it does not consume electricity, and it is easy to use. MagLev, in the current format, has at least two limitations in monitoring polymerization: (i) It cannot monitor polymerization in which there is only a small change in density, $\Delta\rho$. For example, radical polymerization of prepolymers with large molecular weights, and step-growth polymerization involving condensation reactions, in general, have negligible net changes in volume and, therefore, in density. (ii) It is incompatible (in the form we describe here) with processes sensitive to the presence of water because we use an aqueous paramagnetic salt solution to suspend samples of monomers and polymers. (Non-aqueous systems for MagLev are known,^{8,9} but we have not used these here.)

The methodology described in this work will be useful to those concerned with polymerization, especially of hydrophobic vinyl monomers, and for which time, cost, limited sample quantity, portability, and simplicity of operation are important.

Specifically, we believe MagLev could be a potential tool with which to study various aspects of polymerizations (e.g., rates, order of reaction, and inhibitory effects) in both academic and industrially relevant settings: it can (i) screen—rapidly and quantitatively—sensitivities of polymerizations to inhibitors (e.g., O_2 , nitrobenzene, and diphenyl picryl hydrazyl); (ii) investigate the kinetics of polymerization in the presence of solid materials (e.g., particles and fibers), particularly for samples with a high volume ratio of solids (e.g., composite materials); and (iii) examine kinetics of

polymerization for volume-limited samples (1–100 μL), and—with further development—for microscale drops (~ 1 fL to 1 μL) in a format incorporating microfluidic components.

We are developing MagLev as a technique with which to measure the density of diamagnetic materials quantitatively and rapidly.¹⁰ As we normally use it, it requires no more than a pair of NdFeB magnets, a plastic cuvette filled with a liquid paramagnetic medium (e.g., an aqueous solution of MnCl_2 , MnBr_2 , CuSO_4 , FeCl_2 , GdCl_3 , DyCl_3 , or HoCl_3), and a mm-scale ruler (Figure 1 for a schematic, and Supporting

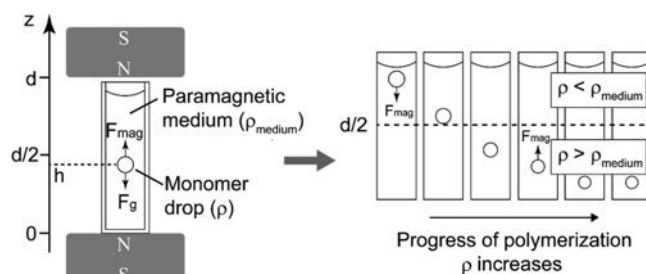


Figure 1. Schematic illustration of a MagLev device used to monitor the change in density for a polymerization reaction. A drop levitates stably in a paramagnetic medium at a levitation height (h) where the magnetic force (F_{mag}) and the buoyancy-corrected gravitational force (F_g) acting on the drop balance each other. When the drop (density ρ) is more dense than the medium (ρ_{medium}), h is less than $d/2$; when the drop is less dense than the medium, h is greater than $d/2$. In both cases, “levitation” means “repulsion of the diamagnetic object from the face of the nearer magnet”. That is, when $\rho > \rho_{\text{medium}}$ (eq 1), levitation acts against the force of gravity and prevents the object from sinking in the paramagnetic medium; when $\rho < \rho_{\text{medium}}$, levitation acts to prevent the object from rising in this medium.

Information, Figure 1S for an actual device used in this study). The magnets are typically positioned coaxially with the like-poles facing; the cuvette is placed in the middle with its vertical axis coaxial with the centerline of the two magnets. A drop of (diamagnetic) liquid monomer levitates in a paramagnetic solution in a magnetic field (we usually use a linear field gradient), provided its density falls in an appropriate range (see below for an explanation for “appropriate”): this levitation reflects a competition between magnetic and buoyant (gravitational) forces. We describe the theory of MagLev in detail elsewhere.¹⁰ Equation 1 gives the levitation height, h (m), of the liquid drop with respect to the surface of the bottom magnet.

$$h = \frac{(\rho - \rho_{\text{medium}})g\mu_0 d^2}{(\chi - \chi_{\text{medium}})4B_0^2} + \frac{d}{2} \quad (1)$$

In this equation, ρ (kg/m^3) is the density of the drop, ρ_{medium} (kg/m^3) is the density of the paramagnetic medium, χ (unitless) is the magnetic susceptibility of the object, χ_{medium} (unitless) is the magnetic susceptibility of the paramagnetic medium, g ($9.8 \text{ m}/\text{s}^2$) is the constant of gravitational acceleration, μ_0 ($4\pi \times 10^{-7} \text{ N}\cdot\text{A}^{-2}$) is the magnetic permeability of the free space, B_0 (T) is the magnetic strength at the surface of the magnets, and d (m) is the distance of separation between the two magnets.

MagLev is a versatile benchtop method that can, with appropriate control of readily accessible variables (e.g., the relative orientation of magnetic and gravitational fields),

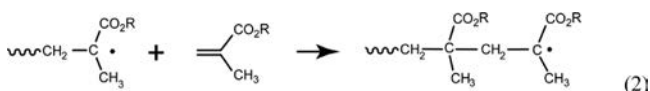
measure the entire range of density observed in matter—from an air bubble ($\rho \approx 0 \text{ g/cm}^3$) to osmium and iridium ($\rho \approx 23 \text{ g/cm}^3$)¹¹—and quantitatively with remarkable resolution ($\Delta\rho \approx 10^{-6} \text{ g/cm}^3$) under appropriately controlled conditions.¹² It also can measure density from samples such as small, irregular solids, heterogeneous objects, gels, or materials with time-dependent density, which may be incompatible with other devices (e.g., pycnometer, oscillating-tube density meter, or densitometer).^{10,13,14}

MagLev of diamagnetic objects in paramagnetic fluids in a magnetic field gradient has found many applications in measurement and use of density. For example, we and others have used it to (i) monitor chemical reactions and binding events on surfaces and in porous matrices,^{15,16} (ii) measure density of living cells, including mammalian cells, yeast, and bacteria,¹⁷ and (iii) perform quality-control of plastic parts.¹⁸

■ EXPERIMENTAL DESIGN

Choice of Polymer Systems. We chose vinyl monomers in this study to demonstrate the utility of MagLev in characterizing the kinetics of polymerizations, because these polymerizations lead to relatively large values of $\Delta\rho$. We used free-radical chain growth polymerization—both thermal polymerization and photopolymerization—with methyl methacrylate (MMA) as a representative polymerization system. Historically, free-radical chain-growth polymerization has been extensively characterized by density-dependent techniques (including dilatometry) because significant differences in the densities of the monomer and the polymer are generally observed in this category of polymerization. For example, the density of MMA and poly(methyl methacrylate) is 0.936 and 1.188 g/mL, respectively, and thus, $\Delta\rho \approx 27\%$ is observed during complete polymerization.

Mechanism and Two Predictions for $\Delta\rho$ of Free-Radical Chain-Growth Polymerization. In free-radical chain-growth polymerization, $\Delta\rho$ is primarily the direct consequence of a decrease in volume as monomers covalently incorporate into the growing polymer chain, and thus, move from a van der Waals distance to a shorter covalent distance. Equation 2 shows an example of radical



polymerization with methacrylate esters. This radical-based mechanism generates two predictions with regard to $\Delta\rho$ that can be experimentally validated using MagLev.

1. *The change in density should be smaller for polymerization of monomers having larger molecular weights (or volumes).* Consider the densities of the monomer ρ_m and of the polymer ρ_p (both calculated on the basis of monomer units in eq 3 and eq 4):

$$\rho_m = \frac{m}{V_m} \quad (3)$$

$$\rho_p = \frac{m}{V_p} = \frac{m}{V_m - \Delta V} \quad (4)$$

In eq 3 and eq 4, m (kg) is the mass of a monomer molecule, V_m (m^3) is the volume occupied on average by a single monomer molecule in liquid monomer (including both the physical volume the monomer molecule occupies and the void space that surrounds it), V_p (m^3) is the volume occupied on average by a single monomeric unit in the polymer, and ΔV (m^3) is the reduction in volume for a single monomer molecule as it incorporates into the polymer chain. eq 5 gives the change in density—expressed as the ratio of the density of the polymer to the monomer to emphasize the change in volume during polymerization.

$$\frac{\rho_p}{\rho_m} = \frac{V_m}{V_m - \Delta V} \quad (5)$$

For polymerization of methacrylate esters, ΔV originates from the addition reaction of the double bonds; its contribution to the overall reduction of the density of the polymer is diluted by its side chains. The larger the side chains of the monomer, the smaller the relative change in density between the polymer and the monomer. We have used three members of the series of n -alkyl methacrylates to validate this prediction experimentally.

2. *The change in density for polymerization by cross-linking chains of a preformed prepolymer approaches zero—i.e., $\Delta\rho \approx 0$.*

A prepolymer can polymerize further to form a larger polymer molecule by cross-linking. When the “monomer” is itself already a polymer, and has a large volume, the relative change in density on further cross-linking is small, i.e., $\Delta\rho \approx 0$. We examined the curing of polydimethylsiloxane (PDMS)—a system in which carbon–carbon double bonds cross-link with silicon hydride bonds on prepolymers using Pt catalysts—to validate this prediction.¹⁹

Choice of the Paramagnetic Medium and Solubility of Monomers and Initiators. Density measurements using MagLev (as conducted here) require the samples to be immersed in a paramagnetic aqueous medium; the experiments, thus, require the monomer and initiator to be insoluble in the paramagnetic medium, and the polymerization to be unaffected by an organic/aqueous interface. In the usual way in which we perform density measurements using MagLev, we use a concentrated (0.5 M) aqueous solution of MnCl_2 as the paramagnetic medium. This solution is paramagnetic, only slightly colored (thus highly transparent for easy visualization), inexpensive, and non-toxic. Hydrophobic monomers and initiators with low solubility in water are, therefore, suitable systems to demonstrate the capabilities of MagLev for characterization of polymerization. Hydrophilic monomers—albeit not the focus of this study—can also be studied using MagLev; they, however, require that the paramagnetic medium be compatible with the hydrophilic monomers or reactive intermediates generated during polymerization. The procedure we used in this paper—a hydrophobic monomer suspended in an aqueous solution of MnCl_2 —would not be directly appropriate for cation or anion polymerizations. These systems might be studied using Gd chelates in hydrophobic solvents⁵ or an inert, flexible container physically separating the monomer from the suspending medium (e.g., a compliant plastic bubble or pouch).²⁰

Choice of MagLev Devices. The MagLev device we used in this study had two indistinguishable NdFeB magnets ($W \times L \times H$: 25.4 mm \times 25.4 mm \times 50.8 mm, poles are on the square faces) positioned 25.0 mm apart with the like-poles facing. (In the Supporting Information, Figure S1 shows an actual device assembled using 3D-printed plastic parts and used in this study.) We chose this specific combination of sizes of magnets and separation distance between the magnets to maximize the strength of the magnetic field on the magnet surface (measured $B_0 \approx 0.51 \text{ T}$) and its gradient in the gap (we used an approximately linear one so that eq 1 applies), and thus to expand the dynamic range of measurable density (the theory is given elsewhere¹¹), while still maintaining a relatively large working distance ($d = 25.0 \text{ mm}$, Figure 1). The device used in this study expanded the range of measurable density—both the low and high limits—using common aqueous paramagnetic solutions (e.g., MnCl_2). The expanded range of density is particularly useful to monitor $\Delta\rho$ of liquid monomers with densities lower than $\sim 1 \text{ g/cm}^3$ (e.g., MMA, 0.936 g/cm^3) (Supporting Information, “Design of the device and alternative approaches”).

■ RESULTS AND DISCUSSION

Change in Density Is Smaller for Polymerization of n -Alkyl Methacrylates with Increasing Volumes of n -alkyl groups. We explored thermal polymerization of MMA, hexyl methacrylate, and octadecyl methacrylate to validate experimentally the prediction that the change in density

Table 1. Densities of Methacrylate Esters and Their Polymers

<i>n</i> -alkyl	ρ_m		ρ_p		$\frac{\rho_{p,est}}{\rho_{m,rep}}$	$\frac{\rho_{p,meas}}{\rho_{m,meas}}$
	reported ^a	measured ^b	estimated ^c	measured ^d		
methyl	0.936	0.928	1.182	1.178	1.26	1.27
hexyl	0.863	0.889	0.974	0.986	1.13	1.11
octadecyl	0.864	0.879	0.917	0.916	1.06	1.04

^aData obtained from www.sigmaaldrich.com for monomers at room temperature. ^bMeasured experimentally; in this study, the densities of monomers using MagLev. ^cDensities of the polymers estimated using eqs 3 and 4, reported densities of the monomers, and a reported ΔV of 22.5 cm³ per mole of monomers. ^dPolymer samples prepared using suspension polymerization at 80 °C. Liquid monomers were used as received (without removal of the inhibitor nor degassing of the liquid), with an aqueous solution of 0.5 M MnCl₂ as the suspending medium and benzoyl peroxide (1 wt%) as the thermal initiator.

should be smaller for polymerization of monomers having larger molecular weights (or volumes) but incorporating a common polymerizable group. We used suspension polymerization (Supporting Information, Figure S3 for details) with these monomers, and obtained small polymer beads (~1 mm). The densities of the monomers and polymers were determined using MagLev and are listed in Table 1. The density of the polymer relative to the monomer, ρ_p/ρ_m , indeed decreased (as expected) with an increasing molecular weight.

This experimental observation can be quantitatively rationalized by simple calculation. Polymerization of *n*-alkyl methacrylates is known to maintain a reasonably consistent reduction in molar volume for each vinyl methacrylate group consumed—it is estimated to be 22.5 cm³/mol—when a monomer in this series polymerizes to yield a polymer;⁷ this consistent reduction in volume originates from the shared chemical moiety (i.e., vinyl group) that participates in the polymerization reaction. Knowing the densities of the monomers in this series (e.g., values reported in the literature) and the reduction in molar volume (22.5 mL/mol) when they are converted to polymers, we estimated the densities of the polymers for several members in this series, and plotted them in Figure 2. Experimental values agree satisfactorily with these estimated densities.

Change in Density for Polymerization of a Prepolymer Approaches Zero As the Preformed Prepolymers Further Cross-Link. We explored the polymerization of a vinyl-containing siloxane prepolymer used in commercial

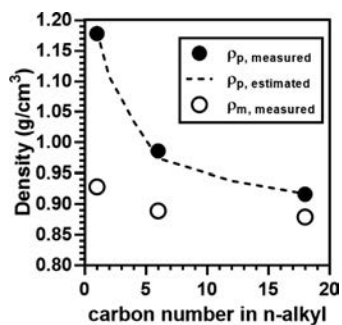


Figure 2. Densities of methacrylate esters and their polymers measured by MagLev. The dotted line represents the estimated densities of the polymers for *n*-alkyl methacrylates (*n* = 1–4, 6, 12, and 18) based on the density values reported in the literature and an assumption of a consistent reduction of molar volume, ΔV , of 22.5 cm³ per mole of monomer molecules that convert completely to polymer.

PDMS products (Dow Corning Sylgard 184) to validate this prediction. The Pt-catalyzed hydrosilylation (the addition reaction of Si–H bonds across olefinic bonds) between prepolymers terminated with vinyl groups and a distinct cross-linking agent having Si–H groups leads to the polymerization of the prepolymers, and yields a final cross-linked (and cured) polymer.¹⁹ Because the change in volume, ΔV , as a result of the hydrosilylation (assuming it is on the same order as that observed in polymerization of *n*-alkyl methacrylates, 22.5 cm³/mol), is much smaller than the bulk volume of the prepolymers (we estimate the molar volume to be ~7300 cm³/mol, assuming a degree of polymerization of 60 and a density of 1.03 g/cm³ for the prepolymer);¹⁹ the change in density (eq 4) when the prepolymers fully polymerize is, therefore, predicted to be minimal ($\rho_p/\rho_m \approx 1.003$) and, in fact, close to the resolution of the device used in this study ($\Delta\rho \pm 0.001$ g/cm³; see Supporting Information, “Treatment of data”, for details). Experimentally, we observed that a drop of un-cross-linked prepolymers levitated at the same height as did a piece of cross-linked PDMS (Figure 3).

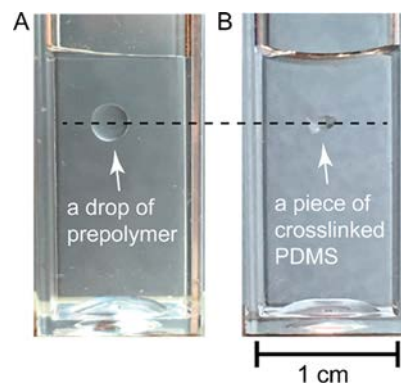


Figure 3. A drop (12.6 μ L) of un-cross-linked prepolymers (A) levitated at the same height as did a small piece of irregular-shaped, cross-linked PDMS (B) in an aqueous solution of 0.5 M MnCl₂.

Characterizing the Kinetics of Thermal Polymerization of MMA. We chose radical polymerization of MMA as our standard polymer system (specifically polymerization thermally initiated by 2,2'-azobis(isobutyronitrile) or AIBN) as our first example, to validate the use of MagLev to characterize the kinetics of its polymerization. We used bulk polymerization using pure monomer of MMA (inhibitors including 4-methoxyphenol and O₂ were removed; see Supporting Information for details) and AIBN to perform the reaction, and focused on the early stage of polymerization to characterize its kinetics. Thermal polymerization of MMA

is a first-order reaction for MMA;²¹ the rate equation takes the form of eq 6:

$$-\frac{d[M]}{dt} = k_p \left(\frac{fk_d[I]}{k_t} \right)^{0.5} [M] \quad (6)$$

In eq 6, $[M]$ (mol/L) is the concentration of the monomer, k_p ($L \text{ mol}^{-1} \text{ s}^{-1}$) is the rate constant of radical propagation, f (unitless) is the efficiency of initiation (that is, the fraction of radicals produced by the homolysis reaction of the initiator that successfully initiate polymer chains), k_d (s^{-1}) is the rate constant of thermal decomposition of the initiator into radicals, $[I]$ (mol/L) is the concentration of the initiator, and k_t ($L \text{ mol}^{-1} \text{ s}^{-1}$) is the rate constant of radical termination.

We carried out polymerization at four temperatures, and measured the density of the reacting mixture every 2 min. We converted the measured density to the concentration of the remaining monomer in the reacting mixture using eq 7 (see Supporting Information, eq S1, for details):

$$[M] = \frac{\rho_m \rho_p}{M_w(\rho_p - \rho_m)} \left[1 - \frac{\frac{1}{\rho_p} + \frac{k_2}{\rho_2}}{\frac{1+k_2}{\rho}} \right] \quad (7)$$

In eq 7, $[M]$ (mol/L) is the concentration of the (remaining) monomer in the polymerizing mixture, ρ_m (g/cm^3) is the density of the monomer, ρ_p (g/cm^3) is the density of the polymer, M_w (g/mol) is the molecular weight of the monomer, k_2 is the mass ratio of the initiator to the monomer in the mixture, ρ_2 (g/cm^3) is the density of the initiator, and ρ (g/cm^3) is the density of the reacting mixture.

We determined the initial rates of polymerization over the first 6 min during which we monitored the polymerization (Figure 4). We estimated the Arrhenius activation energy of this polymerization under the conditions described here to be 79 kJ/mol, which falls in the reported range of 62.0–84.9 kJ/mol (determined using independent techniques, including dilatometry and differential scanning calorimetry, under similar conditions).²²

Characterizing the Kinetics of Photopolymerization of MMA. We performed photopolymerization of MMA directly in the MagLev device by levitating a single drop of monomer mixture (inhibitors including 4-methoxyphenol and O_2 are removed; see Supporting Information for details) containing a hydrophobic photoinitiator (2,2-dimethoxy-2-phenylacetophenone) in an aqueous MnCl_2 solution (0.5 M, purged with Ar), and then irradiating the drop using UV light (365 nm from a hand-held Hg lamp). The change in density $\Delta\rho$ (we presume, entirely due to polymerization) was measured continuously as reaction proceeded. Photopolymerization has five advantages over thermal polymerization as a model system with which to study polymerization using MagLev: it (i) enables real-time measurements of density; (ii) provides a nearly isothermal environment (especially for the small drops) because the aqueous paramagnetic medium effectively acts as an isothermal bath; (iii) simplifies sample preparation; (iv) consumes small quantities ($\sim 1\text{--}50 \mu\text{L}$) of sample; and (v) enables rapid experiments. The experiments we describe here involving photopolymerization were all conducted at room temperature, and in the presence of an aqueous solution of MnCl_2 , and are thus analogous to suspension polymerization.

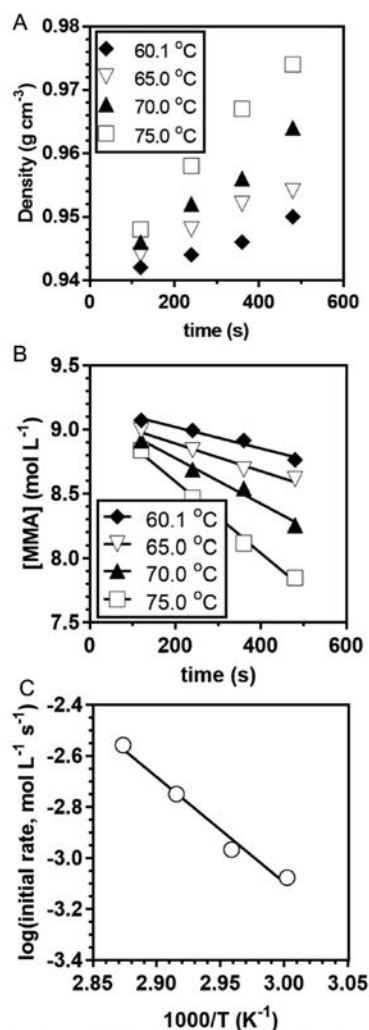


Figure 4. Determination of the Arrhenius activation energy of thermally initiated polymerization of MMA using AIBN. We monitored the changes in density of the polymerizing mixture (pure MMA with 1.3 wt% AIBN,) over time by transferring small ($\sim 2 \mu\text{L}$), cooled aliquots of the reacting mixture to the MagLev device (A), converted the measured densities to the changes in the concentrations of the remaining monomer in the reacting mixture, performed linear fitting to estimate the initial rates of polymerization (B), and plotted the initial rates of polymerizations with respect to the temperatures under which the polymerizations were performed (C). [MMA] stands for the concentration of MMA in the reacting mixture. $N = 1$ for all experiments.

We first validated the expected behavior of photopolymerization of pure MMA by subjecting the levitated drop to continuous or periodic UV irradiation. (It would be ideal to include standards of density in the same cuvette during experiment as an external control; we, however, did not implement this approach because the polymerizing drop would traverse nearly the entire height of the cuvette in this experiment.) We converted the measured density to the fractional conversion of the monomer, x , in the reacting mixture using eq 8 (see Supporting Information, Table S2 for details and Figure S7 for independent validation using ^1H NMR):

$$x = \frac{\rho_m \rho_p}{\rho_p - \rho_m} \left[\left(\frac{1}{\rho_m} + \frac{k_2}{\rho_2} \right) - \frac{1 + k_2}{\rho} \right] \quad (8)$$

When the UV light was kept on throughout the reaction (Figure 5A), the rate of conversion increased slowly for the

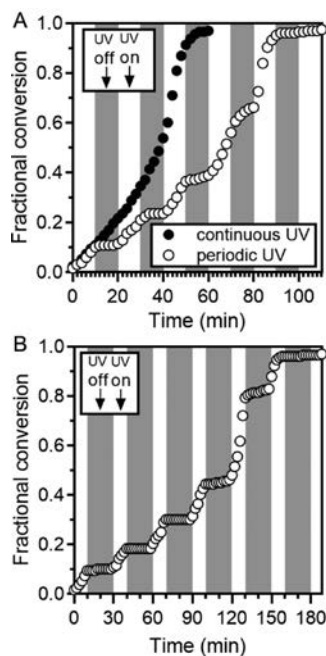


Figure 5. Use of MagLev to monitor the progress of photopolymerization. (A) A drop ($\sim 10 \mu\text{L}$) of pure MMA with photoinitiator, 2,2-dimethoxy-2-phenylacetophenone (5 wt%), was levitated in an aqueous solution of 0.5 M MnCl_2 , and irradiated using a continuous (dark circles) or periodic (white circles, 10 min of dark period for every 10 min of irradiation) UV light (365 nm from a Hg lamp). The fractional conversion of MMA in the polymerizing drop was calculated using the density of the drop measured from its levitation height. (B) The drop was irradiated using a periodic UV light with longer dark periods (20 min for every 10 min of irradiation).

first 20 min, and then more rapidly starting at ~ 30 min, and finally reached plateau at ~ 60 min (at which time, the drop had converted to a solid sphere). This behavior—auto-acceleration in polymerization of MMA—is a well-known effect: the Trommsdorff effect, or simply the “gel effect”. It is caused by the slowing rate of diffusion-limited termination of the propagating radicals by radical–radical combination as the viscosity of the reaction mixture increases. We emphasize that this auto-acceleration is unlikely to have originated from the heat generated locally by the polymerizing drop since the small drop ($\sim 10 \mu\text{L}$, ~ 2.7 mm in diameter) was thermally stabilized in a comparatively large quantity of aqueous solution (~ 2.5 mL; see Figure S10 for measurement of temperature of a polymerizing drop). The smallest drop we tested ($1.1 \mu\text{L}$, ~ 1.3 mm in diameter) showed the same behavior (Supporting Information, Figure S11). When the UV irradiation was periodically blocked (Figure 5A, open circles, 10 min of dark periods followed by 10 min of irradiation), the polymerization was nearly halted (e.g., at ~ 10 min) or slowed significantly. The residual polymerization during the dark periods in the gel region (e.g., 50–60 min and 70–80 min) suggests that the propagating radicals persisted in the reacting

mixture (in the absence of additional radicals generated by UV irradiation), and did not recombine completely (likely due to the increasing viscosity of the reacting mixture). In a second experiment, we increased the dark periods to 20 min, twice the length of UV irradiation (10 min), and observed that the residual polymerization persisted similarly, albeit with a reduced magnitude, in the dark periods during the gel region (e.g., 100–120 min and 130–150 min).

We established a theoretical model to describe the average rate of polymerization for a drop. This model incorporated three key steps of radical polymerization (radical initiation, propagation, and termination) and the profile of absorbed UV light (i.e., Beer’s law) as light traverses a sphere (see Supporting Information for derivation). Equation 9 gives the derived equation for the average rate of polymerization of a spherical drop.

$$-\frac{d[M]}{dt} = k_p[M] \left(\frac{\alpha[A]\phi 10^3 I_0}{k_t} \right)^{0.5} \times \left[\frac{3}{\alpha[A]R} \left(\frac{1}{2} + \frac{e^{-\alpha[A]R}}{\alpha[A]R} + \frac{e^{-\alpha[A]R} - 1}{(\alpha[A]R)^2} \right) \right] \quad (9)$$

$$K' = \left[\frac{3}{\alpha[A]R} \left(\frac{1}{2} + \frac{e^{-\alpha[A]R}}{\alpha[A]R} + \frac{e^{-\alpha[A]R} - 1}{(\alpha[A]R)^2} \right) \right] \quad (10)$$

In eq 9, k_p ($\text{L mol}^{-1} \text{s}^{-1}$) is the rate constant for propagation, k_t ($\text{L mol}^{-1} \text{s}^{-1}$) is the rate constant for radical termination, $[M]$ (mol L^{-1}) is the concentration of monomer, $[A]$ (mol L^{-1}) is the concentration of initiator, R (m) is the radius of the drop, α is the absorption coefficient of A ($\text{L mol}^{-1} \text{cm}^{-1}$, $\alpha = \epsilon \ln 10$, where ϵ is molar absorptivity), ϕ (unitless) is the quantum yield for initiation (the number of propagating chains initiated per light photon absorbed), and I_0 ($\text{mol cm}^{-2} \text{s}^{-1}$) is the incident light intensity at the surface of the drop. Equation 10 describes the correction term K' which corrects for the shape effect of the spherical drop in absorbing UV light. This term approaches unity when the traversing UV irradiation is minimally attenuated by the sample drop, i.e., $\alpha[A]R \approx 0$ (a small drop or low concentrations of photoinitiator or both; see Supporting Information, eqs S14–S16, for details).

We performed three sets of experiments to validate the theoretical predictions. We used eq 11 as the general formula to determine experimentally the orders of reaction for the monomer and the initiator in the polymerization (i.e., the values of a and b). We then compared them to the theoretical values described in eq 9.

$$-\frac{d[M]}{dt} = kK'[M]^a[A]^b \quad (11)$$

In this equation, K' is the correction term (eq 10), and k is a parameter that, according to eq 9, depends on the conditions of irradiation and the types of photoinitiator and monomer used.

Determination of the Order of Reaction for the Monomer. We determined the order of reaction for the monomer experimentally by measuring the initial rates of polymerization at different concentrations of monomer, but using the same concentration of the photoinitiator. (We used the same procedures described in the caption of Figure 5.) We chose anisole as a diluent (the range of initial $[MMA]$ is

1.2–9.4 M) in this experiment because it is a suitable solvent for polymerization of MMA,^{23,24} and has a density, 0.993 g/cm³, similar to that of the monomer MMA, 0.936 g/cm³, so that we could use the same aqueous MnCl₂ solution to measure the densities of drops containing varying volumetric ratios of anisole and MMA. We converted the experimentally determined levitation heights of the drops to densities (Figure 6A), and then to concentrations of the monomer in the drops

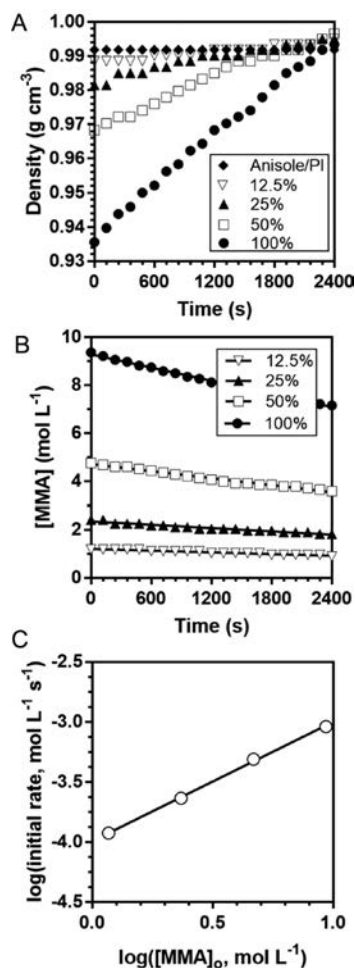


Figure 6. Determination of the order of reaction for MMA in photopolymerization using MagLev. MMA was diluted in anisole and the initial concentrations (v%) of MMA in the mixtures were indicated in the figures. All drops were $\sim 10 \mu\text{L}$ and contained the same concentration of photoinitiator (PI), 2,2-dimethoxy-2-phenylacetophenone, 0.27 wt%. The increase in the density of the drop over time (A) was converted to the decrease in the concentration of the monomer (B). Initial rates of polymerization were estimated using the slopes of the linear fits in (B), and replotted in (C). [MMA] stands for the concentration of MMA in the reacting mixture, and $[\text{MMA}]_0$ is the initial concentration. $N = 1$ for all experiments.

(Figure 6B) using eq 7. We observed that the change in the concentration of the monomer over time was approximately linear up to ~ 40 min, and therefore, used this range of data to estimate the initial rates of polymerization. Linear fit of the log–log plot of the initial rates vs the monomer concentrations (eq 11, kK' is a constant in this case) shows the slope of the line is 0.993, which suggests that the order of reaction for MMA in this photopolymerization is ~ 1.0 . The

experimental value agrees with the theoretical prediction in eq 9

Determination of the Order of Reaction for the Photoinitiator. We used a similar approach to determine the order of reaction for the photoinitiator in this photopolymerization. We measured the initial rates of polymerization (Figure 7A) in the first 10 min for drops ($\sim 10 \mu\text{L}$)

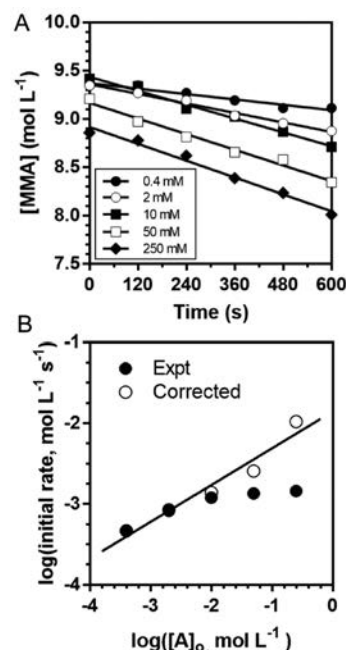


Figure 7. Determination of the order of reaction for photoinitiator using MagLev. Initial rates of polymerization were estimated using the slopes of the linear fits in (A), and replotted in (B) as filled circles. The rates of polymerization were corrected for the effect of UV absorbance in the sample drop using eq 10 (open circles), and the first two points overlapped completely with the ones without correction. All drops had $\sim 10 \mu\text{L}$ volumes and contained different concentrations of photoinitiator, 2,2-dimethoxy-2-phenylacetophenone (0.4–250 mM), in pure MMA. [MMA] stands for the concentration of MMA in the reacting mixture, and $[\text{A}]_0$ stands for the initial concentration of the initiator. $N = 1$ for all experiments.

containing different concentrations of photoinitiator (0.4–250 mM) in pure MMA. The experimentally determined initial rates of polymerization increased to a plateau when the concentrations of photoinitiator increased (Figure 7B). We also replotted the initial rates by correcting for shape effects of the drop absorbing UV light—i.e., dividing both sides of eq 11 by the correction factor K' (which we calculated from experimentally determined values of α , $[\text{A}]$, and R as described in eq 10) to remove the effect of light attenuation in the sample drop. The corrected initial rates are approximately linear ($R^2 = 0.95$) on a log–log plot of the corrected initial rates vs the concentrations, and the estimated order of reaction for the photoinitiator in this polymerization is 0.46. This experimental value agrees with the theoretical value, 0.5 (eq 9).

3. Evaluation of the Dependence of the Rate of Polymerization on the Size of the Drop. The rate of polymerization depends on the size of the drop unless the UV irradiation is not significantly attenuated across the sample drop. A large drop experiences more light attenuation across the drop than a small drop does and, therefore, has a

comparatively smaller overall rate of polymerization under the same conditions. The correction term K' (eq 10) quantitatively describes this size-dependent effect, and we performed experiments to validate this prediction.

We measured the rates of polymerization of sample drops that differ only in size (~ 1 – $50 \mu\text{L}$), and found that the initial rates of polymerization decreased as the drop size increased, as expected qualitatively. We then corrected for size-dependent effects by measuring the sizes of the drops, and calculating the corresponding values of the correction terms. The corrected initial rates of polymerization should, in principle, be independent of the sizes, and thus, fall on a horizontal line when plotted against the volumes of the drops. Figure 8B shows that the corrected initial rates, in fact, still

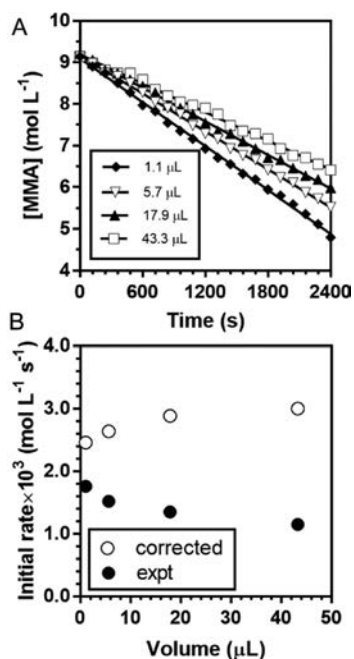


Figure 8. Dependence of the rate of polymerization on the size of the drop. The initial rates of polymerization of the sample drops were determined using linear fits (A) and replotted in (B) as filled circles. The corrected initial rates of polymerization were plotted as open circles. All drops contained the same concentration (50 mM) of photoinitiator, 2,2-dimethoxy-2-phenylacetophenone, in pure MMA. The sample drop spanned the entire range of volume accessible under the conditions reported in this study (using pipets and standard cuvettes with a 10 mm path length).

show a weak dependence on the drop sizes. This observation may originate from causes such as (i) the inhibitory effects of the residual dissolved O_2 in the suspending medium or (ii) possible rotation of the drops during polymerization; we did not investigate these causes in this study. Overall, the experimental results agreed semiquantitatively with the theoretical predictions.

Thermal Polymerization in the Presence of an Included Solid. Polymerization in the presence of a suspended solid may be difficult, and in some cases impractical, to study using common techniques. For example, it is difficult to monitor polymerization of a thin liquid film of a monomer on a particulate support (such as small beads or particles), or polymerization of a monomer impregnated in a porous matrix (such as carbon or glass fibers).

We used thermal polymerization of MMA in the presence of a porous, non-woven fabric at room temperature initiated by the reaction of benzoyl peroxide and 4,*N,N*-trimethylaniline, as an example, to demonstrate the capability of MagLev to characterize these types of samples. We specifically selected three representative, non-woven fabrics commonly used in composite materials (to enhance mechanical properties) based on aramid fiber ($\rho = 1.39 \text{ g/cm}^3$, determined by MagLev in this study), carbon fiber ($\rho = 1.73 \text{ g/cm}^3$), and glass fiber ($\rho = 2.52 \text{ g/cm}^3$). We monitored the changes in density of the monomer-impregnated discs (3 mm in diameter, prepared using a biopsy punch), and thus, the progress of polymerization in the presence of a solid. We focused on the early stages of polymerization (Figure 9A), in part because (i) the

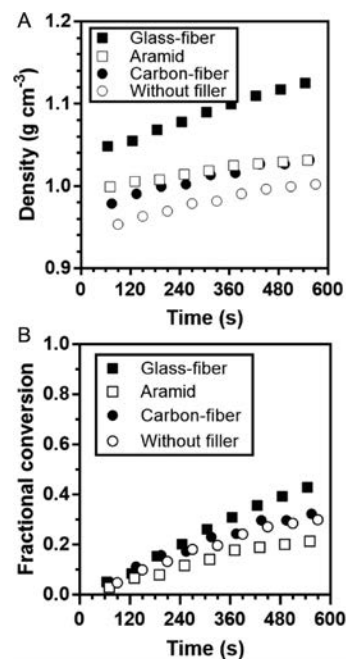


Figure 9. MagLev to monitor polymerization in the presence of a solid. (A) The changes in density over time of a polymerizing drop and three 3 mm discs impregnated with a polymerizing mixture. The polymerizing mixture contained MMA (inhibitor not removed), benzoyl peroxide (4.6 wt%) and 4,*N,N*-trimethylaniline (4.9 wt%). The suspending medium was an aqueous solution of MnCl_2 1.0 M. (B) The calculated fractional conversion of MMA in the drop and in the discs over time. $N = 1$ for all experiments.

polymerization proceeded most rapidly during the first 10 min and (ii) the influence of the finite solubility of the components (e.g., MMA and 4,*N,N*-trimethylaniline) in the suspending medium was small over a short time period. (the dissolution of the lighter components in the mixture would raise the apparent density of the disc, and therefore, artificially increase the fractional conversion.)

We calculated the fractional conversion (Supporting Information, eq S1) of the monomer MMA in the absence and presence of an included solid (Figure 9B). The fractional conversion for the sample of glass fiber deviated the most from the sample containing the reacting mixture alone; this deviation might be in part accounted for by the largest difference in the density of glass fibers (2.52 g/cm^3) from the reacting mixture (0.94 g/cm^3) among the three types of materials examined—a slight dissolution of the reacting

components would cause the largest (artificial) change in fractional conversion. We did not, in this study, attempt to investigate the detailed causes of discrepancy of the kinetics of polymerization (e.g., the influence of the type of materials or of the coatings on them on the kinetics of polymerization); we focused on the demonstration of MagLev in monitoring and characterizing polymerization in these complex, heterogeneous samples, and of its compatibility with three distinct classes of fibers commonly used in composite materials. This demonstration also points to options of improvements in experimental protocols with which to perform and monitor polymerization in the presence of solid materials using MagLev (e.g., pre-saturation of the suspending medium with participating chemicals).

■ CONCLUSIONS

Polymer science has developed a number of instrument tools and analytical techniques to characterize the kinetics of polymerization. There remains an unmet need—particularly in the early stages of studies of polymers—for simple, convenient, broadly applicable analytical techniques to characterize a range of types of samples with different physical properties (e.g., liquids, gels, pastes, solids), and to study polymerization in heterogeneous, opaque, or irregularly shaped samples. This work demonstrates that MagLev is a versatile method with which to characterize free-radical polymerization of water-insoluble, low-molecular-weight monomers in complex samples. MagLev characterizes the basic types of thermal polymerizations and photopolymerizations of methacrylate-based monomers. It is also compatible with irregularly shaped, quantity-limited, heterogeneous composite materials (we demonstrated this capability using small, porous, and non-transparent fabrics impregnated with liquid of MMA)—a type of analysis that would otherwise be difficult to perform.

MagLev, in the form as we have developed in this study, is best applied to water-insoluble, low-molecular-weight monomers that undergo radical polymerization and show a significant change in density during polymerization. Free-radical polymerization of MMA is a representative example. While we focused on the common types of radical polymerizations (i.e., thermal polymerization and photopolymerization of methacrylate monomers), the technique can be extended in a straightforward manner to study polymerization involving cross-linkable monomers (e.g., ethylene glycol dimethyl methacrylate), two or more monomers (e.g., copolymerization), and advanced processes of polymerization, such as certain types of atom-transfer radical polymerization. For example, MagLev should be, in principle, compatible with living-radical photopolymerization of methacrylates using water-compatible catalysts.²⁵ MagLev, as developed, will not readily work, for example, for ring-opening polymerization using Grubbs's catalysts and norbornene (0.87 g/cm³) as monomer because (i) the maximal change in density associated with the polymerization is small (the density of polynorbornene is ~0.96 g/cm³), and (ii) the polymerization is performed in solvents which further dilute the already small changes in density. Other variants of MagLev, such as the configuration optimized for high-sensitivity measurement of density,¹² may be adapted for studies of polymerization that require resolving subtle changes in density.

MagLev complements the set of tools available to polymer and materials scientists who wish to measure density as a tool for investigating processes or characterizing materials. The particular strengths of this technique lie in its simplicity in use, ease with which it can be maintained, and broad compatibility with different types of samples (including heterogeneous and composite materials). The weakness of MagLev as described in this study, compared to other techniques, is its exclusive measurement of a physical property of a polymerizing sample; MagLev does not provide chemical information regarding polymerization (e.g., molecular weight of the polymer or the polydispersity index, linear or branched or cross-linked structures of the polymer chains). MagLev is a non-destructive technique, and the samples could be easily retrieved for downstream chemical analyses or for observation over long periods of time. Given these useful characteristics—particularly the simplicity and the broad accessibility to users in different settings—we believe MagLev should find a number of applications in investigating mechanisms of polymerization, evaluating sensitivities of polymerization to inhibitors, and studying polymerization in the presence of solids for studies of composite materials. It also has the simplicity required for educational use, and for field and quality-control work.

■ ASSOCIATED CONTENT

📄 Supporting Information

The Supporting Information is available free of charge on the ACS Publications website at DOI: 10.1021/jacs.7b10901.

Detailed experimental procedures, comparison of MagLev and ¹H NMR, measurement of temperature of a polymerizing drop, and additional supporting materials, including Tables S1 and S2 and Figures S1–S11 (PDF)

■ AUTHOR INFORMATION

Corresponding Author

*gwhitesides@gmwgroup.harvard.edu

ORCID

George M. Whitesides: 0000-0001-9451-2442

Notes

The authors declare no competing financial interest.

■ ACKNOWLEDGMENTS

This work was funded by the U.S. Department of Energy, Office of Basic Energy Sciences, Division of Materials Sciences and Engineering under award number ER45852. Specifically, the DOE grant supported the design of the MagLev device and its use to perform density measurements for polymerizations. S.N.S. acknowledges the Simons Foundation for salary support; A.A.N. thanks the Swiss National Science Foundation mobility fellowship for funding; J.M. acknowledges a Canadian fellowship from Fonds de Recherche Nature et Technologies; D.C.C. acknowledges the Gates Foundation for salary support; L.Y. acknowledges NSF award CHE-1506993 for salary support. We thank Jonathan W. Hennek and Alex Nemiroski for helpful discussions at the early stages of the study, and Daniel Preston for discussions on temperature measurement of small liquid drops.

■ REFERENCES

- (1) Alb, A. M.; Drenski, M. F.; Reed, W. F. *Polym. Int.* **2008**, *57*, 390–396.
- (2) Hoogenboom, R.; Fijten, M. W. M.; Abeln, C. H.; Schubert, U. S. *Macromol. Rapid Commun.* **2004**, *25*, 237–242.
- (3) Zoller, P. *Encyclopedia of Polymer Science and Technology*; John Wiley & Sons, Inc.: 2013 (online).
- (4) Abbey, K. J. In *Emulsion Polymers and Emulsion Polymerization*; Bassett, D. R., Hamielec, A. E., Eds.; American Chemical Society: Washington, DC, 1981; Vol. 165, pp 345–356.
- (5) Bradbury, J. H. *J. Chem. Educ.* **1963**, *40*, 465.
- (6) Martín, O.; Mendicuti, F.; Tarazona, M. P. *J. Chem. Educ.* **1998**, *75*, 1479.
- (7) Patel, M. P.; Braden, M.; Davy, K. W. *Biomaterials* **1987**, *8*, 53–56.
- (8) Bwambok, D. K.; Thuo, M. M.; Atkinson, M. B.; Mirica, K. A.; Shapiro, N. D.; Whitesides, G. M. *Anal. Chem.* **2013**, *85*, 8442–8447.
- (9) Mirica, K. A.; Phillips, S. T.; Mace, C. R.; Whitesides, G. M. *J. Agric. Food Chem.* **2010**, *58*, 6565–6569.
- (10) Mirica, K. A.; Shevkoplyas, S. S.; Phillips, S. T.; Gupta, M.; Whitesides, G. M. *J. Am. Chem. Soc.* **2009**, *131*, 10049–10058.
- (11) Nemiroski, A.; Soh, S.; Kwok, S. W.; Yu, H. D.; Whitesides, G. M. *J. Am. Chem. Soc.* **2016**, *138*, 1252–1257.
- (12) Nemiroski, A.; Kumar, A. A.; Soh, S.; Harburg, D. V.; Yu, H. D.; Whitesides, G. M. *Anal. Chem.* **2016**, *88*, 2666–2674.
- (13) Lockett, M. R.; Mirica, K. A.; Mace, C. R.; Blackledge, R. D.; Whitesides, G. M. *J. Forensic Sci.* **2013**, *58*, 40–45.
- (14) Atkinson, M. B.; Bwambok, D. K.; Chen, J.; Chopade, P. D.; Thuo, M. M.; Mace, C. R.; Mirica, K. A.; Kumar, A. A.; Myerson, A. S.; Whitesides, G. M. *Angew. Chem., Int. Ed.* **2013**, *52*, 10208–10211.
- (15) Mirica, K. A.; Phillips, S. T.; Shevkoplyas, S. S.; Whitesides, G. M. *J. Am. Chem. Soc.* **2008**, *130*, 17678–17680.
- (16) Shapiro, N. D.; Mirica, K. A.; Soh, S.; Phillips, S. T.; Taran, O.; Mace, C. R.; Shevkoplyas, S. S.; Whitesides, G. M. *J. Am. Chem. Soc.* **2012**, *134*, 5637–5646.
- (17) Durmus, N. G.; Tekin, H. C.; Guven, S.; Sridhar, K.; Arslan Yildiz, A.; Calibasi, G.; Ghiran, I.; Davis, R. W.; Steinmetz, L. M.; Demirci, U. *Proc. Natl. Acad. Sci. U. S. A.* **2015**, *112*, E3661–3668.
- (18) Hennek, J. W.; Nemiroski, A.; Subramaniam, A. B.; Bwambok, D. K.; Yang, D.; Harburg, D. V.; Tricard, S.; Ellerbee, A. K.; Whitesides, G. M. *Adv. Mater.* **2015**, *27*, 1587–1592.
- (19) Lisensky, G. C.; Campbell, D. J.; Beckman, K. J.; Calderon, C. E.; Doolan, P. W.; Ottosen, R. M.; Ellis, A. B. *J. Chem. Educ.* **1999**, *76*, 537.
- (20) McGinniss, V. D.; Holsworth, R. M. *J. Appl. Polym. Sci.* **1975**, *19*, 2243–2254.
- (21) Odian, G. *Principles of polymerization*, 4th ed.; John Wiley & Sons, Inc.: Hoboken, NJ, 2004.
- (22) Armitage, P. D.; Hill, S.; Johnson, A. F.; Mykytiuk, J.; Turner, J. M. C. *Polymer* **1988**, *29*, 2221–2228.
- (23) Bamford, C. H.; Brumby, S. *Makromol. Chem.* **1967**, *105*, 122.
- (24) Olaj, O. F.; Schnoll-Bitai, I. *Monatsh. Chem.* **1999**, *130*, 731–740.
- (25) Fors, B. P.; Hawker, C. J. *Angew. Chem., Int. Ed.* **2012**, *51*, 8850–8853.